Effective linearization by noise addition in threshold detection and implications for stochastic optics

2000 J. Phys. A: Math. Gen. 33 3997

(http://iopscience.iop.org/0305-4470/33/22/304)

J. Phys. A: Math. Gen. **33** (2000) 3997–4007. Printed in the UK PII: S0305-4470(00)09379-3

Effective linearization by noise addition in threshold detection and implications for stochastic optics

Sue Sulcs†, Graham Oppy† and Barry C Gilbert‡

† Department of Philosophy, Monash University, Wellington Road, Clayton, 3168, Australia
‡ Telstra Research Laboratories, 770 Blackburn Road, Clayton, 3168, Australia

E-mail: b.gilbert@trl.oz.au

Received 8 November 1999

Abstract. We present some computer simulation results pertaining to the restoration of a weak sinusoidal input signal after threshold detection with additive random noise. We show how, if stochastic optics is regarded as a viable theory, these results may cast doubt upon some conclusions drawn from seven experimental realizations of the Einstein–Podolsky–Rosen thought experiment performed between 1982 and 1998.

1. Introduction

Recently there have been a number of papers published on stochastic resonance, which is the amplification of weak but regular signals by strong random additive noise [1, 2]. The main idea of this is simple, but clever.

Many kinds of signal detection in engineering and science involve thresholds. That is, only signals with moduli above some minimum level are detected, and the remaining feeble signals are rejected. Indeed, Wiesenfeld and Moss [1] state 'In practice all detectors have a minimum threshold; inputs smaller than this are "invisible" '. An electronic device that models this kind of function is a comparator. If another electronic device called a pulse-stretcher (or monostable multivibrator) is connected in series with a comparator, then we have a system that can convert an analogue (continuous) input signal to a quantized (0, 1) output pulse. The output pulse has a fixed amplitude and width, and is either present or absent. Two of us put forward this electronic model in [3] (see figure 1). Suppose now that we present a series of Gaussian pulses, with slowly varying periodic sinusoidal modulation, as the input signal to the threshold detector in figure 1, and average the series of output pulses, as in figure 2(*a*). We find that the resultant averaged signal has a shape unlike the input modulation. It is just a rectangular wave. However, the outcome is different if we add random noise to the regular signal at the input, just before the comparator, as in figure 2(*b*). We attempted this with uniformly distributed noise, and with Gaussian noise. Noise addition boosts some low-amplitude Gaussian pulses over the threshold, and thus makes it possible for them to give rise to output pulses. When noise is added to high-amplitude signal pulses, there are more output pulses than in the low-level region of the envelope. After many output pulses have been recorded, over many cycles of the modulation, the series is averaged, and this time we observe an analogue waveform. Observations of this kind can be found in [1] and references therein.

0305-4470/00/223997+11$30.00

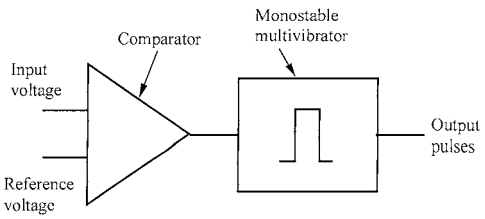

Figure 1. Threshold detection system consisting of a comparator and a monostable multivibrator (pulse-stretcher). When the input voltage to the comparator exceeds the comparator's predetermined threshold setting, the pulse-stretcher outputs a pulse of amplitude and width that can be set in advance, otherwise, there is no output.

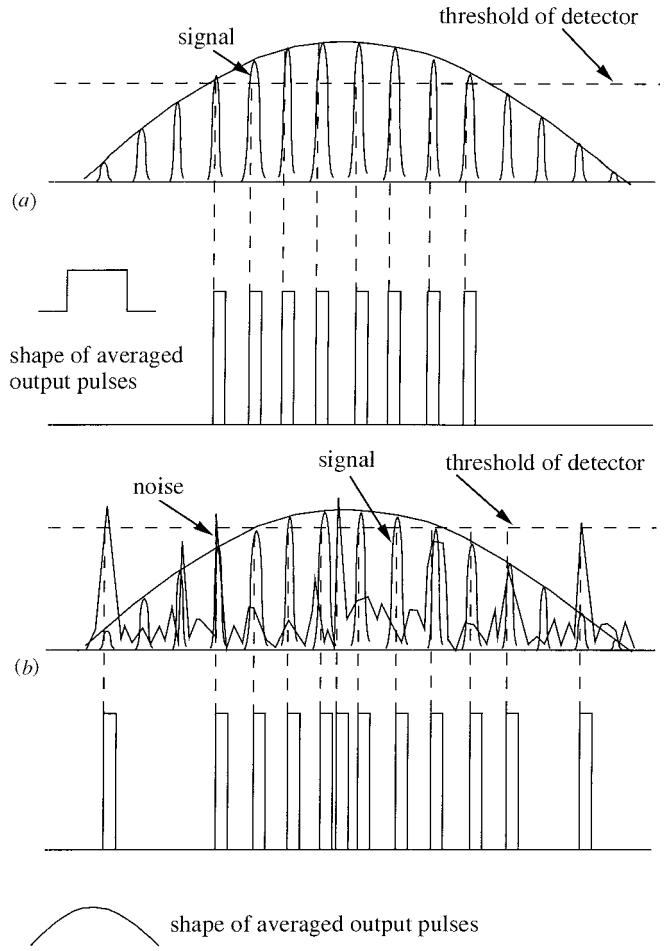

Figure 2. A train of positive Gaussian pulses modulated by a slowly varying sinusoidal envelope is input to the comparator in figure 1, which is a threshold detector. (*a*) Pulses output by the system in the hypothetical case of zero additive noise at the comparator input. When many series of pulses are averaged, the result will be a rectangular wave. (*b*) Pulses output by the system when there is some additive noise at the comparator input. When many series of pulses are averaged, the result will be a curve of some kind. The conditions under which this curve reproduces the input sinusoidal envelope are discussed in section 1.

In some of the work reported in [1] there is little or no freedom to vary the threshold level, which is sometimes set well above the signal, and the problem then is to discover how much noise to add at the input to optimize the output signal-to-noise ratio (SNR). In some

cases the noise level to be added greatly exceeds the signal level. In [1], a formula for such an optimization is given. The term 'stochastic resonance' has been used to refer to a wide range of situations, and some of these are not amenable to time averaging. For those that are, we suspected that for periodic input signals there would exist circumstances for which the output SNR could potentially tend to infinity if the averaging time tends to infinity. This would correspond to recovering the input modulation with negligible harmonic distortion. We were interested in discovering *how much* random noise would have to be added to the signal in order to restore the input modulation, after averaging, without harmonic distortion. Our modelling is aimed at clarifying quantum optical systems, in which the output SNR should be kept as high as possible, but there is considerable scope in varying both threshold and SNR, e.g. using a pulse-height discriminator, cooling photomultiplier tubes (PMT) or diodes, and varying the anode voltage (of the PMT) or the reverse breakdown voltage (of the diode). We assumed for the modelling that the threshold level is constrained only by a minimum of the RMS signal voltage. For single-photon levels at centre frequency ν, this corresponds to an energy density per unit frequency interval of $\frac{1}{2}h\nu$ multiplied by some function of the frequency (see below). Given complete freedom in varying the threshold except for this constraint, we found by trial that a necessary condition for recovering the signal modulation waveform is SNR $\leqslant 1$. (Once set, the threshold must, of course, remain constant for each run in the simulation.) In other words, only if the RMS noise voltage exceeds, or at least equals, the RMS signal voltage, is it possible for the waveform resulting from averaging the output pulses to have the same shape as the input waveform. For real-time sampling, the well established Nyquist criterion must be respected. In our modelling, this criterion was met, i.e. the highest frequency present in the noise was at least twice the frequency of the signal modulation envelope. However, in principle the Nyquist rate is not necessary given sufficient time averaging. The higher the threshold, the higher the level of the added noise required, and the longer the averaging process takes. If the output waveform matches the input modulation, then by Fourier theory it follows that the input and output have the same frequency spectrum, and the system is functioning effectively as a *linear* system. Let us use the phrase 'effective linearization' to describe what has been achieved by the addition of random noise. This process is related to, but distinct from, the smoothing via 'dithering' and 'stochastic linearization' mentioned in [1]. By adding random noise to a signal in an inherently nonlinear detection process, and averaging the digital output pulses, we achieve the same result as if we had used a linear detector in the first place.

2. Stochastic optics and the Bell inequalities

As pointed out in [1, 2] threshold detectors are common in natural processes, including biological ones. Within standard quantum theory (QT), light detection is not thought to involve a threshold. This is because within that theory, both the electromagnetic field and the energy levels of matter are quantized. PMT data sheets indicate that the output count rate is linear with respect to input light intensity. A few stalwart 'local realists' within the physics community question some of the orthodox (Copenhagen) interpretation of QT, especially quantum non-separability and the quantization of the field [4–7].

There is a famous thought experiment called the Einstein–Podolsky–Rosen (EPR) experiment [8]. We discovered 23 experimental realizations of this experiment, performed up to 1998 [9–30], of which the earliest [9] does not involve a test of a Bell-type inequality. The EPR experiment is considered to be a crucial experiment that can decide between QT and the deterministic or local realistic (hidden-variable) theories. Some variant of Bell's inequality [31], which is a prediction of local realism, is compared with the experimental observations. All

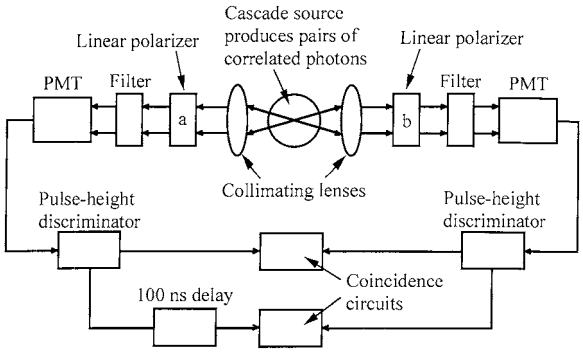

Figure 3. Apparatus used in a two-channel photon coincidence counting EPR experiment carried out by Aspect *et al* [19]. (Figure after [19].)

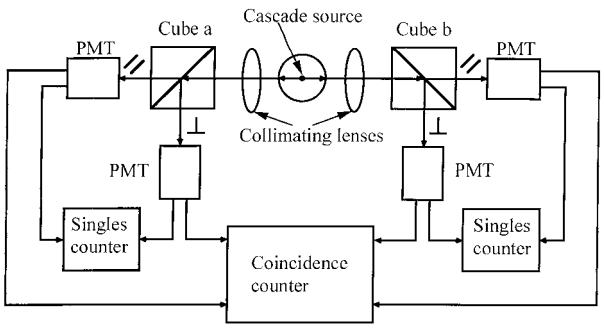

Figure 4. Apparatus used in four-channel EPR experiment carried out by Aspect *et al* [20]. (Figure after [20].)

but one of the EPR realizations have used light rather than massive particles. Two experiments [11, 12] agreed with local realism. See figures 3 and 4 for a typical set-up with two and four channels, respectively. The experiment calls for light of extremely low intensity, i.e. the full-width at half-maximum (FWHM) of the photons (wavepackets) $\ll$ photon mean separation. This should hold everywhere on the optical path, including immediately after the source. Some of the local realistic theories are termed stochastic optics or stochastic electrodynamics (SED) [5, 6, 32–34]. In some of these theories the field is not quantized, and the so-called zero-point field (ZPF), or quantum noise, is a real field, whereas in QT it is merely virtual. In SED, the fluctuating ZPF replaces the uncertainty of QT. There is an equilibrium between the radiation entering the ZPF from atoms, and the radiation absorbed by them, so energy conservation is not violated. The energy density of the ZPF per unit frequency interval is believed to be given by

$$u(\nu) = (8\pi\nu^2/c^3)\tfrac{1}{2}h\nu. \tag{1}$$

If we suppose the field to be unquantized, but matter quantized (such theories are often called 'semiclassical') then when radiation is incident upon a detector (an absorbing atom) the Planck unit of energy, equal to Planck's constant h times the frequency ν, provides a natural intensity threshold. We are not referring to the well known frequency threshold; in fact, in optical EPR experiments the light was filtered to ensure that only light of the relevant frequency could impinge on each detection system. If the intensity threshold did not exist, then without a signal being emitted, even low noise peaks, including thermal

noise, the fluctuating zero-point field, and other noise, would be detected, whereas there is evidence that only the high peaks are detected (called 'dark counts'). However, could we not reconcile a zero-level threshold with the observation of relatively few dark counts by postulating that there do not happen to be many ZPF or thermal fluctuations? The answer is no. The spectra of both thermal noise and ZPF are well established (the first by measurement as well as theory, the second only by theory, including an assumption of Lorentz invariance), and these spectra imply the swamping of all measurements by dark counts in the absence of any threshold. For instance, photographic film would eventually become completely exposed in a dark container. Marshall and Santos [5] and Marshall [6] discuss the threshold notion. Thus, from the point of view of stochastic optics (which *inter alia* it is the aim of the EPR experiment to test), light detection has a threshold nature. Moreover, in low-intensity optical experiments there is often a piece of apparatus called a pulse-height discriminator. The output of a PMT or diode is not usually quantized [35], a fact which is usually attributed to 'noise'. The discriminator standardizes (quantizes) the output. This introduces further nonlinearity and gives greater freedom in changing the overall threshold level.

Although the received view is that local realism is already conclusively refuted, the pure Bell inequality, which is derived from local realism alone, has never been tested. Additional assumptions have been made in every case. In particular, in [20, 25–30], in which optical frequency light was used as a source, a very strong assumption was made. (In [26, 27, 30] a violation of Bell's inequality was inferred but was not the primary aim of the experiment.) This assumption is often called 'faithful sampling', but in the case of [20] it is pointed out [36] that the assumption made was the Garuccio–Rapisarda (GR) assumption [37]:

> For every photon in the state λ, the sum of the detection probabilities in the ordinary and in the extraordinary beams emerging from a two-way polarizer does not depend on the polarizer's orientation.

This assumption would not be fulfilled if there were threshold effects, because if light emissions of different amplitudes impinge on the detector, a threshold would bias the detection in favour of the higher-level emissions. Light of different amplitudes (with a sinusoidal variation) would arise classically if the emission passes through a polarizer at various angles as in [20, 28, 29] or in an interference experiment as in [25–27, 30].

3. The CHSH inequality and the GR modification

In the following, the vectors $\boldsymbol{a}$, $\boldsymbol{b}$, $\boldsymbol{a}'$ and $\boldsymbol{b}'$ are the directions of polarizers relative to some given direction. With regard to the two-channel experiment (figure 3) $R(\boldsymbol{a}, \boldsymbol{b})$ refers to the coincidence rate with the first polarizer at angle $\boldsymbol{a}$ and the second at $\boldsymbol{b}$. In the four-channel experiment (figure 4), the symbol $R_{++}(\boldsymbol{a}, \boldsymbol{b})$, etc is used, where the + and − subscripts refer to the cases of polarization parallel to and perpendicular to the optic axis of a given polarizing cube, respectively.

The Clauser–Horne–Shimony–Holt (CHSH) inequality is derived from local realism with a weak additional assumption [38, 39]. This inequality is

$$-1 \leqslant [R(\boldsymbol{a}, \boldsymbol{b}) - R(\boldsymbol{a}, \boldsymbol{b}') + R(\boldsymbol{a}', \boldsymbol{b}) + R(\boldsymbol{a}', \boldsymbol{b}') - R(\boldsymbol{a}', \infty) - R(\infty, \boldsymbol{b})]/R_0 \leqslant 0 \qquad (2)$$

$\boldsymbol{a}$, $\boldsymbol{b}$, $\boldsymbol{a}'$, and $\boldsymbol{b}'$ are usually chosen to be 0°, 22.5°, 45° and 67.5°, respectively, to some given direction. The R's are long-run coincidence detection rates which are taken to be equivalent

to probabilities, and the symbol ∞ signifies taking out a polarizer on one side. R_0 is the coincidence rate with both polarizers removed.

Freedman [10, 39] showed that (2) reduces to a simpler form when the experiment is rotationally invariant

$$\delta = |R(22.5^\circ) - R(67.5^\circ)|/R_0 - \tfrac{1}{4} \leqslant 0 \tag{3}$$

where the angles in the arguments refer to the relative angle between the two polarizers. This is called the Freedman inequality.

The GR inequality is a modification of the CHSH inequality

$$-2 \leqslant S \leqslant 2 \tag{4}$$

where S is given by

$$S = E(\boldsymbol{a}, \boldsymbol{b}) - E(\boldsymbol{a}, \boldsymbol{b}') + E(\boldsymbol{a}', \boldsymbol{b}) + E(\boldsymbol{a}', \boldsymbol{b}') \tag{5}$$

and E by

$$E(a, b) = \frac{R_{++}(a, b) + R_{--}(a, b) - R_{+-}(a, b) - R_{-+}(a, b)}{R_{++}(a, b) + R_{--}(a, b) + R_{+-}(a, b) + R_{-+}(a, b)}. \tag{6}$$

For simplicity, in the present paper we consider only experiments that are rotationally invariant. The matters at issue do not depend on non-rotationally invariant cases.

Predictions of various linear theories for the two-channel experiment (figure 3) can usually be stated in the following parametrized form, where $\phi = |\boldsymbol{a} - \boldsymbol{b}|$:

$$\frac{R(\phi)}{R_0} = \alpha[1 + \beta \cos(2\phi)]. \tag{7}$$

For a four-channel experiment (figure 4)

$$\frac{R_{++}(\phi)}{R_0} = \frac{R_{--}(\phi)}{R_0} = \alpha[1 + \beta \cos(2\phi)] \tag{8}$$

$$\frac{R_{+-}(\phi)}{R_0} = \frac{R_{-+}(\phi)}{R_0} = \alpha[1 - \beta \cos(2\phi)]. \tag{9}$$

Substituting equations (8) and (9) into equation (6), we obtain for the above-mentioned angles, $E = (\boldsymbol{a}, \boldsymbol{b}) = E(\boldsymbol{a}', \boldsymbol{b}) = E(\boldsymbol{a}', \boldsymbol{b}') = \frac{1}{2}\sqrt{2}\beta$ and $E(\boldsymbol{a}, \boldsymbol{b}') = -\frac{1}{2}\sqrt{2}\beta$, so by (5)

$$S = 2\sqrt{2}\beta \tag{10}$$

and $-2 \leqslant 2\sqrt{2}\beta \leqslant 2$, by (4). It is apparent that the GR inequality is constrained by β but not by α, so multiplying all the coincidence rates in equation (6) by a constant scaling factor has no effect on the correlation coefficient E.

Substituting (7) into (3) we obtain $\delta = |\alpha\beta\sqrt{2}| - \frac{1}{4} \leqslant 0$, so that the Freedman inequality (3) is constrained by both α and β.

It is clear that the GR inequality does not constrain local realism as rigorously as does the CHSH inequality.

4. Computer simulation of the EPR experiment

We carried out a rotationally invariant simulation of the experiment of [19]. This is more complex than the single-channel simulation discussed in section 1, because a coincidence window is involved. The assumptions made were local realistic, e.g. that light propagates according to Maxwell's equations, even at or below single-photon intensity. The detection system modelled on each channel is that in figure 1 and the photons are represented by the Gaussian pulses in figure 2, i.e. the magnitudes of the envelopes of Gaussian wavepackets with the optical frequency wave omitted. The modulation envelope is sinusoidal with respect to angle, but not time. The mean photon separation is 20 × FWHM with a pseudo-Poissonian train of wavepackets. Results of an earlier, similar, simulation were presented in [3]. In the present version, the polarization angle of each pair of emitted photons is a continuous variable and is uniformly random in time.

Questions raised by readers of [3] suggest that we gave the impression that the coincidence-counting simulation consists of numerical integration of the kind

$$p_{12}(\phi, T, W_c) = \int \mathrm{d}\theta\, \rho(\theta) p_1(\theta) p_2(\phi - \theta) g(W_c) \tag{11}$$

where T is the threshold, W_c is the width of the coincidence window, ϕ is as defined in section 3 and the single-channel detection probability $p_j(\theta|T)$ is given by

$$p_j(\theta|T) = \int \mathrm{d}N_j\, \rho(N_j) f(T, (N_j + V_0 \cos\vartheta)^2) \tag{12}$$

where N_j is the noise voltage on the jth channel, with density $\rho(N_j)$, V_0 is the signal maximum voltage and θ is the polarization angle of the emission. This is an abbreviated representation of our model, but we simulated the experiment of figure 3 in a complex sequential series of steps, some of which are nonlinear. In order to calculate the coincidence probability we did not begin with a single detection probability calculation such as (12). The program counts coincidences, assuming independent random Gaussian noise sources exist at the inputs to each PMT. The simulated noise is meant to represent any kind of noise that could affect the counting rates, e.g. thermal, zero-point or dynode noise, but we modelled an ideal source that produces no unpaired transition photons.

Although the program was written with many adjustable parameters, the only parameters we varied in the present work were the threshold level and the polarizer orientation. An increase in the threshold in our simulation gives rise to a downward shift of the whole curve, and vice versa (see figure 5). This is similar to changing the discriminator threshold in a real experiment. Simulation affords wider scope in parameter control than exists in real experiments. However, the raw data (prior to accidental subtraction) in [19] are consistent with curve (a) and the data in [40] are consistent with curve (b) (see section 5). For all the data in figure 5, the SNR ≈ 2 and W_c was set a little greater than the wavepacket FWHM. The adjustable parameters were chosen by trial and error to produce an almost sinusoidal output in reasonable computer time. The threshold values are noted in the caption to figure 5 and remained constant for each set of relative polarizer orientations (i.e. each curve). See the appendix for curve-fitting details. We only simulated figure 3, but we can apply the same set of results to the experiment of figure 4, in which the polarizers were not removed for normalization. (We have more information than we need for the experiment of figure 4.) In figure 4, on each side of the experiment, ideally the total incident intensity must split between the parallel and perpendicular beams, so the intensities of the two beams are proportional to $\cos^2\theta$ and $\sin^2\theta$. Since $\cos\phi = \sin(90^\circ \pm \phi)$, it follows that

$$R_{++}(\phi) = R_{--}(\phi) = R_{+-}(90^\circ - \phi) = R_{-+}(90^\circ - \phi). \tag{13}$$

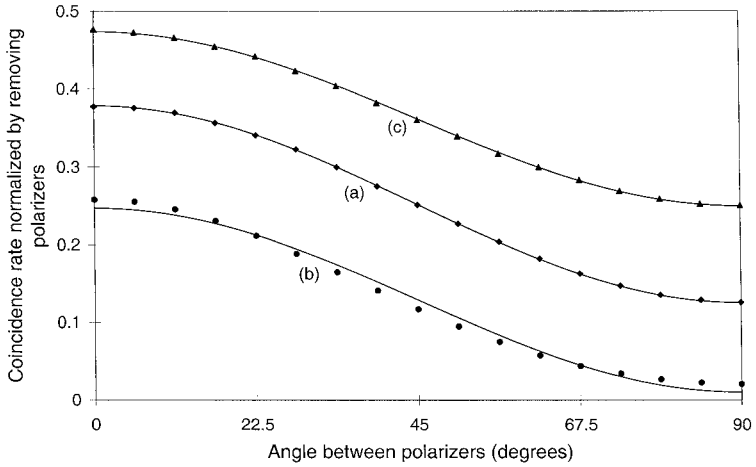

Figure 5. Normalized coincidence rates for the EPR experiment calculated by computer simulation. The simulation is based on the set-up used by Aspect *et al* [19]. The threshold settings relative to the signal maximum of 1 V were (a) 1.4 V, (b) 1.81 V, (c) 1.27 V. The full curves are sinusoidal fits to the data. When correlation coefficients corresponding to figure 4 are calculated from two relevant points in (b), the GR inequality is significantly violated without background subtraction. All three curves satisfy the Freedman inequality.

Here are the salient points of the simulation. First, almost a pure sinusoid (figure 5 curve (a)) is shown to be the long-run output of a nonlinear threshold detection system with the addition of random noise (which is of mathematical interest, apart from optics). This is such a good sinusoid that many readers of [3] believed we had not simulated the experiment at all, but had merely evaluated the following integral:

$$p_{12}(\phi) = \frac{1}{\pi}\int_0^{\pi} \mathrm{d}\theta \cos^2(\theta)\cos^2(\phi-\theta)$$
$$= 0.25[1 + 0.5\cos(2\phi)] \tag{14}$$

which does not differ from figure 5 (curve (a)) very noticeably. Secondly, even when there is some noticeable harmonic distortion (figure 5, curve (b)) the vertical offset outweighs the harmonic distortion by over an order of magnitude, and the increase in parameter β between (a) and (b) is significant. The modelling indicates that changing the discriminator threshold level can alter the situation from one of agreement with the GR inequality (4)–(6) to one of significant disagreement with it. Parameter S in equation (5) is worked out for the case of figure 5 (curve (b)) in the appendix. This violation of the GR inequality occurs without any background subtraction. All three curves in figure 5 satisfy the Freedman inequality, which is a more reliable test of local realism since the additional assumption made in its derivation is much weaker.

5. The shortage of published raw data

We have noted that figure 5 (curve (b)), which violates the GR inequality without background subtraction, has some harmonic distortion. QM predicts in ideal cases a sinusoid of the form (7), with $\alpha = 0.25$ and $\beta = 1$. Aspect and Grangier published some extra data [40] which demonstrate a violation of the GR inequality without accidental coincidence subtraction. However, they only reported additional data at two relative polarizer angles,

which is insufficient to determine whether an undistorted sinusoid would have been obtained. Since the polarizers were not removed in order to normalize the coincidence rates, we cannot know whether the relevant $R(\phi)/R_0$ curve would have been offset downwards from the centre as in figure 5 (curve (b)). The two are consistent given the data available. It has been argued [33, 36] that accidental subtraction results in an unreliable test of Bell's inequalities. Apparently the only experiment to violate the more stringent Freedman and CHSH inequalities without subtracting accidental coincidences is [10], although the data actually graphed in [10], in which harmonic distortion is low, appear to be the result of accidental subtraction. The distortion level is higher in [22]. Subtraction of accidentals cannot affect distortion; it only vertically lowers the coincidence-rate curve (consequently E in equation (6) increases) and increases the peak-to-peak range of the rates when they are normalized. Our modelling suggests that coincidence rates from which accidentals are subtracted should be sinusoidal as in figure 5 curve (a). Some reports [23, 28] of parametric down-conversion experiments do not make clear whether accidentals were subtracted or not. They were not subtracted in [29], but in that report only four out of 16 graphs are published. In any event it has been shown [41] that down-conversion experiments [23–30] are generally unreliable for testing Bell's inequalities. The publication of more raw data would be useful; the presently published data are, on balance, consistent with our simulation.

6. Concluding remarks

The next step in this research is to find either an analytical proof of, or a counter example to, the criterion reported in section 1 for the undistorted restoration of an input function after passing through a nonlinear threshold detector. The conclusions drawn from seven experimental tests of Bell's inequalities have been questioned as a result of simulation based on the addition of random noise. Although these experiments have almost certainly refuted some local realistic theories, we have demonstrated that there is a plausible way in which the so-called 'detection loophole' [42, 43] remains open. Until now it was thought that only within artificial conspiracy theories, according to which circumstances conspire to favour QT although the world is really deterministic, was there any kind of local realistic response to the EPR experiments.

Acknowledgments

We are grateful to Professors Michael Morgan and John Bigelow, Ian P Macfarlane, Steve Iskra and Caroline H Thompson for useful discussions. We also thank two anonymous referees. S Sulcs acknowledges support from the Commonwealth of Australia.

Appendix. Detail of curve fitting for figure 5 and violation of the GR inequality using figure 5, curve (b)

Sinusoidal curve-fitting results for figure 5. See equation (7):

(a)	$\alpha = 0.2519$	$\beta = 0.5025$	$\chi^2 = 5 \times 10^{-6}$
(b)	$\alpha = 0.1288$	$\beta = 0.9191$	$\chi^2 = 1.2 \times 10^{-3}$
(c)	$\alpha = 0.3620$	$\beta = 0.3086$	$\chi^2 = 1.6 \times 10^{-5}$.

Standard deviations of simulated points:

(a) $\sigma = 0.0005$

(b) $\sigma = 0.007$

(c) $\sigma = 0.001$.

For the simulated points in figure 5, curve (b), the program was run until the number of coincidences counted with both polarizers removed was 5.01×10^5.

Calculation of error in S due to harmonic distortion in figure 5, curve (b): the equation to the best-fit sinusoid is $p = \alpha[1+\beta\cos(2\phi)]$ from (7). Therefore, $\mathrm{d}p = \mathrm{d}\alpha+(\alpha\,\mathrm{d}\beta+\beta\,\mathrm{d}\alpha)\cos(2\phi)$ where $\mathrm{d}p = 0.007$.

Considering $\phi = \pi/4$ and 0, we get $\mathrm{d}\alpha = \mathrm{d}p = 0.007$, and $0 = \alpha\,\mathrm{d}\beta + \beta\,\mathrm{d}\alpha$,

$$\therefore |\mathrm{d}\beta| = 0.919 \times 0.007/0.129 = 0.050 \qquad \text{and} \qquad \beta = 0.92 \pm 0.05.$$

$S = (2\sqrt{2})\beta = 2.60 \pm 0.14$ which violates inequality (4) by over four standard deviations.

References

[1] Wiesenfeld K and Moss F 1995 *Nature* **373** 33

[2] Moss F and Wiesenfeld K 1995 *Sci. Am.* **273** 50

[3] Gilbert B C and Sulcs S 1996 *Found. Phys.* **26** 1401

[4] Selleri F (ed) 1988 *Quantum Mechanics Versus Local Realism: the Einstein–Podolsky–Rosen Paradox* (New York: Plenum) p 18

[5] Marshall T W and Santos E 1988 *Found. Phys.* **18** 185
Marshall T W and Santos E 1997 The myth of the photon *The Present Status of the Quantum Theory of Light* ed S Jeffers, S Roy, J-P Vigier and G Hunter (Dordrecht: Kluwer) pp 67–77

[6] Marshall T W 1988 Stochastic electrodynamics and the Einstein–Podolsky–Rosen argument *Quantum Mechanics Versus Local Realism: the Einstein–Podolsky–Rosen Paradox* (New York: Plenum) pp 413–32

[7] Lamb W E Jr 1995 *Appl. Phys.* B **60** 77

[8] Einstein A, Podolsky B and Rosen N 1935 *Phys. Rev.* **47** 777
d'Espagnat B 1976 *Conceptual Foundations of Quantum Mechanics* 2nd edn (Reading, MA: Benjamin) pp 75ff
Squires E J 1994 *The Mystery of the Quantum World* 2nd edn (Bristol: IOP Publishing) pp 84–98
Mandel L and Wolf E 1995 *Optical Coherence and Quantum Optics* (Cambridge: Cambridge University Press) pp 648–57

[9] Kocher C A and Commins E D 1967 *Phys. Rev. Lett.* **18** 575

[10] Freedman S J and Clauser J F 1972 *Phys. Rev. Lett.* **28** 938

[11] Holt R A and Pipkin F 1973 *Harvard University Preprint* unpublished

[12] Faraci G, Gutkowski D, Notarrigo S and Pennisi A R 1974 *Lett. Nuovo Cimento* **9** 607

[13] Kasday L R, Ullman J D and Wu C S 1975 *Nuovo Cimento* B **25** 633

[14] Clauser J F 1976 *Phys. Rev. Lett.* **36** 1223

[15] Fry E S and Thompson R C 1976 *Phys. Rev. Lett.* **37** 465

[16] Lamehi-Rachti M and Mittig W 1976 *Phys. Rev.* D **14** 2543

[17] Wilson A R, Lowe J and Butt D K 1976 *J. Phys. G: Nucl. Phys.* **2** 613

[18] Bruno M, d'Agostino M and Maroni C 1977 *Nuovo Cimento* B **40** 143

[19] Aspect A, Grangier P and Roger G 1981 *Phys. Rev. Lett.* **47** 460

[20] Aspect A, Grangier P and Roger G 1982 *Phys. Rev. Lett.* **49** 91

[21] Aspect A, Dalibard J and Roger G 1982 *Phys. Rev. Lett.* **49** 1804

[22] Perrie W, Duncan A J, Beyer H J and Kleinpoppen H 1985 *Phys. Rev. Lett.* **54** 1790
For 1986 experiments by Hassan T H, Duncan A J, Perrie W, Beyer H J and Kleinpoppen H see 1988 *Quantum Mechanics Versus Local Realism: the Einstein–Podolsky–Rosen Paradox* (New York: Plenum) p 198

[23] Shih Y H and Alley C O 1988 *Phys. Rev. Lett.* **61** 2921

[24] Ou Z Y and Mandel L 1988 *Phys. Rev. Lett.* **61** 50

[25] Rarity J G and Tapster P R 1990 *Phys. Rev. Lett.* **64** 2495

[26] Kwiat P G, Steinberg A M and Chiao R Y 1993 *Phys. Rev.* A **47** R2472

[27] Tapster P R, Rarity J G and Owens P C M 1994 *Phys. Rev. Lett.* **73** 1923

[28] Kwiat P G, Mattle K, Weinfurter H, Zeilinger A, Sergienko A V and Shih Y 1995 *Phys. Rev. Lett.* **75** 4337
[29] Weihs G, Jennewein T, Simon C, Weinfurter H and Zeilinger A 1998 *Phys. Rev. Lett.* **81** 5039
[30] Tittel W, Brendel J, Gisin B, Herzog T, Zbinden H and Gisin N 1998 *Phys. Rev.* A **57** 3229
[31] Bell J S 1964 *Physics* **1** 195
Clauser J F and Horne M A 1974 *Phys. Rev.* D **10** 526
[32] Boyer T H 1984 *Phys. Rev.* D **29** 1096
[33] Santos E 1985 Stochastic electrodynamics and the Bell inequalities *Open Questions in Quantum Physics* ed G Tarozzi and A van der Merwe (Dordrecht: Reidel) pp 283–96
[34] de la Peña L and Cetto A M 1996 *The Quantum Dice: an Introduction to Stochastic Electrodynamics* (Dordrecht: Kluwer)
[35] Munroe D M 1980 *Recovering Signals from Noise and Special Measurement Problems Involving Low Level Radiation* (Princeton, NJ: EG&G Princeton Applied Research)
[36] Santos E 1992 *Phys. Rev.* A **46** 3646
[37] Garuccio A and Rapisarda V A 1981 *Nuovo Cimento* A **65** 269
[38] Clauser J F, Horne M A, Shimony A and Holt R A 1969 *Phys. Rev. Lett.* **23** 880
[39] Clauser J F and Shimony A 1978 *Rep. Prog. Phys.* **41** 1881
[40] Aspect A and Grangier P 1985 *Lett. Nuovo Cimento* **43** 345
[41] Santos E 1996 *Phys. Lett.* A **212** 10
[42] Pearle P M 1970 *Phys. Rev.* D **2** 1418
[43] Thompson C H 1996 *Found. Phys. Lett.* **9** 357